



## Pathway to a molecular calcium methyl†

 Cite this: *Chem. Commun.*, 2024, 60, 7882

 Kyle G. Pearce,<sup>id</sup>\* Samuel E. Neale,<sup>id</sup> Claire L. McMullin,<sup>id</sup> Mary F. Mahon and Michael S. Hill<sup>id</sup>

 Received 18th June 2024,  
 Accepted 2nd July 2024

DOI: 10.1039/d4cc02930e

rsc.li/chemcomm

The dimeric  $\beta$ -diketiminato calcium hydride, [(BDI)CaH]<sub>2</sub> (BDI = HC{(Me)CN-2,6-*i*Pr<sub>2</sub>C<sub>6</sub>H<sub>3</sub>})<sub>2</sub>), reacts with ZnMe<sub>2</sub> to afford the bimetallic calcium zincate complex, [(BDI)Ca( $\mu$ -CH<sub>3</sub>)<sub>2</sub>Zn( $\mu$ -H)]<sub>2</sub>, which subsequently undergoes an intramolecular reaction to effect the formation of [(BDI)CaMe]<sub>2</sub>, a notable omission from the homologous series of  $\beta$ -diketiminato arylcalcium derivatives.

Since the discovery of Grignard reagents in 1900,<sup>1</sup> organomagnesium derivatives have prevailed as some of the most widely employed compounds in chemical synthesis. In contrast, exploration of magnesium's heavier congener, calcium, lay largely dormant throughout the 20th Century, to the extent that it has even been deemed as the "sleeping beauty" of organometallic chemistry.<sup>2</sup> Despite reports of  $\sigma$ -C-Ca-bonded calcium alkyl and aryl complexes from as early as 1905,<sup>3,4</sup> the first crystallographically verified calcium  $\sigma$ -alkyl, [Ca{CH(SiMe<sub>3</sub>)<sub>2</sub>}(Diox)]<sub>2</sub> (Diox = 1,4-dioxane), was only reported by Cloke and Lappert in 1991.<sup>5</sup> Like this species, many subsequently characterised diorganocalcium compounds were dependent on the use of silylated and kinetically stabilising organic anions.<sup>6</sup> More recently, however, a defined and characteristic chemistry has finally started to emerge for derivatives of wholly hydrocarbon ligands.<sup>2</sup> Especially notable in this regard are routes to a variety of di- and monoaryl calcium reagents and dimethylcalcium devised, respectively, by the groups of Westerhausen and Anwander.<sup>7,8</sup>

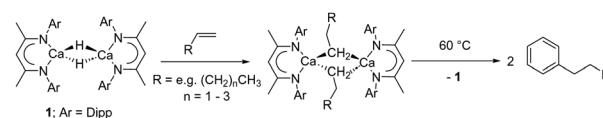
While sufficiently remarkable to merit a mononymic account of its synthesis,<sup>8</sup> the subsequent reactivity of [CaMe<sub>2</sub>]<sub>∞</sub> in the absence of secondary donors is relatively limited as a consequence of its polymeric nature and consequent poor solubility in non-coordinating media.<sup>8</sup> Further advancements

have, thus, focused on heteroleptic derivatives,<sup>9</sup> with the  $\beta$ -diketiminate ligand scaffold proving a particularly adept, hydrocarbon-soluble spectator anion.<sup>10</sup> While  $\sigma$ -*n*-alkyl species had previously proved inaccessible *via* the analogous THF-adducted hydride, [(BDI)Ca(THF)H]<sub>2</sub> (BDI = HC{(Me)CN-2,6-*i*Pr<sub>2</sub>C<sub>6</sub>H<sub>3</sub>})<sub>2</sub>),<sup>11</sup> its base-free variant, [(BDI)CaH]<sub>2</sub> (**1**),<sup>12</sup> was found to be reactive toward terminal alkenes to provide a wide range of dimeric  $\sigma$ -*n*-alkyl derivatives, [(BDI)Ca(R)]<sub>2</sub> (Scheme 1).<sup>13</sup> While a further impact of reduction in coordinative saturation at the calcium centre was manifest in the ability of such  $\sigma$ -alkyls to effect the nucleophilic alkylation of benzene (Scheme 1),<sup>12</sup> a similar alkene insertion-based approach is clearly inapplicable to the synthesis of the simplest methylcalcium homologue.

We have recently developed a transmetallation-based approach to prepare coordinatively unsaturated  $\sigma$ -aryl derivatives.<sup>14,15</sup> Sequential reactions with arylmercuric reagents (Ar<sub>2</sub>Hg; Scheme 2) enabled the preparation of [(BDI)Ca( $\mu$ -H)( $\mu$ -Ar)Ca(BDI)] and [(BDI)Ca( $\mu$ -Ar)( $\mu$ -Ar')Ca(BDI)] (Ar = C<sub>6</sub>H<sub>5</sub>, *ortho*-Me-C<sub>6</sub>H<sub>5</sub>, *meta*-Me-C<sub>6</sub>H<sub>5</sub>, *para*-Me-C<sub>6</sub>H<sub>5</sub>, 3,5-*t*Bu<sub>2</sub>C<sub>6</sub>H<sub>3</sub>, Ar' = C<sub>6</sub>H<sub>5</sub>, *ortho*-Me-C<sub>6</sub>H<sub>5</sub>, *meta*-Me-C<sub>6</sub>H<sub>5</sub>, *para*-Me-C<sub>6</sub>H<sub>5</sub>). These  $\beta$ -diketiminato arylcalcium derivatives detail a structural dependence between  $\eta^1$ - and  $\eta^6$ -aryl coordination and facilitate uncatalyzed access to biaryl molecules by direct S<sub>N</sub>Ar displacement of halide from aryl bromides. While a similar mercury-based approach could be applicable to the preparation of a molecular calcium methyl complex, [(BDI)CaMe]<sub>2</sub>, and our previous use of arylmercurials was a necessary synthetic expedient, the severe toxicity of dimethylmercury renders this synthetic pathway unattractive.<sup>16</sup> In this contribution, therefore, we describe the

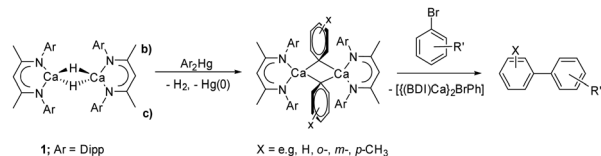
Department of Chemistry, University of Bath, Claverton Down, Bath, UK.

E-mail: kgp29@bath.ac.uk

 † Electronic supplementary information (ESI) available: General synthetic experimental details, NMR spectra, X-ray analysis of compound **3** and **4**. CCDC 2360310 and 2360311. For ESI and crystallographic data in CIF or other electronic format see DOI: <https://doi.org/10.1039/d4cc02930e>


**Scheme 1** Preparation of calcium *n*-alkyl complexes from compound **1** and the nucleophilic alkylation of benzene.





**Scheme 2** Use of compound **1** in the synthesis of arylcalcium compounds and the reaction of the phenyl derivative with aryl bromides to prepare biaryl molecules.

use of the less-toxic group 12 metal, zinc, to address this lacuna in the homologous chemistry of  $\beta$ -diketiminato alkylcalcium derivatives.

Immediate analysis by  $^1\text{H}$  NMR spectroscopy of a reaction of compound **1** with one equivalent of  $\text{ZnMe}_2$  (1.0 M in heptane) in  $d_8$ -toluene, identified three upfield shifted methyl resonances at  $\delta_{\text{H}}$   $-0.71$ ,  $-0.81$  and  $-1.39$  ppm (Fig. S1, ESI $^\dagger$ ). The secondmost downfield of these signals was assigned to  $[(\text{BDI})\text{ZnMe}]$  (**2**),<sup>17</sup> which, accompanied by the appearance of a colourless precipitate, continued to emerge as the sole soluble component of the reaction over the subsequent 16 hours (Fig. S2, ESI $^\dagger$ ). Repetition of this reaction with two equivalents of  $\text{ZnMe}_2$  afforded **2** over a shorter time period (4 hours), albeit the methyl-containing species at  $\delta_{\text{H}}$   $-1.39$  ppm was again observed to form but be subsequently consumed. In an attempt to trap the other methyl organometallic intermediates formed during this reaction, **1** was again reacted with two equivalents of  $\text{ZnMe}_2$  but immediately placed in the freezer ( $-35$  °C). This procedure afforded a crop of colourless crystals of **3**. Analysis of **3** by  $^1\text{H}$  NMR spectroscopy evidenced a single  $\beta$ -diketiminate environment characterized by a BDI  $\gamma$ -methine singlet at  $\delta_{\text{H}}$  4.77 ppm and an associated upfield signal at  $\delta_{\text{H}}$   $-0.66$  ppm, which resonated with a respective 1:6 ratio of intensities by relative integration. A further ( $1\text{H}$ ) singlet at 3.15 ppm was tentatively identified as a hydride signal, the incorporation of which alongside the apparent retention of both methyl groups of the zinc reagent was interpreted to imply a bimetallic structure. This inference was subsequently confirmed by single crystal X-ray diffraction analysis, which identified compound **3** as  $[(\text{BDI})\text{Ca}(\mu\text{-CH}_3)_2\text{Zn}(\mu\text{-H})]_2$  (Fig. 1).

The asymmetric unit of **3** contains two independent, but effectively identical, dimer halves and the following representative discussion refers only to the Ca1-containing molecule. Complex **3** provides Ca1 with two N–Ca contacts [2.3237(17) and 2.3253(16) Å], such that, in a manner reminiscent of the puckered geometry observed for  $[(\text{BDI})\text{Ca}(\text{o-C}_2\text{B}_{10}\text{H}_{11})]$  and  $[(\text{BDI})\text{CaN}(\text{SiMe}_3)_2]$ ,<sup>18–20</sup> the calcium centre is situated *ca.* 1.088 Å above the least squares plane defined by the BDI-backbone. Ca1 is connected to Zn1 through a three-centre methyl-bridged bond, exhibiting Ca1–C30 and Zn1–C30 bond lengths of 2.608(2) and 2.038(2) Å, respectively. These distances are in line with the only other reported Ca– $\mu_2$ –C–Zn species,  $[(\text{THF})_2\text{Ca}\{\mu\text{-CH}_2\text{SiMe}_3\}_2\text{Zn}(\text{CH}_2\text{SiMe}_3)_2]$  (Ca–C 2.655(2), Zn–C 2.080(2) Å), reported by Westerhausen in 2002.<sup>21</sup> The bridging hydrides display a significant asymmetry with respect to each calcium atom such that Ca1–H1<sup>1</sup> is elongated by *ca.* 1 Å



**Fig. 1** Molecular structure of the Ca1-containing component of **3**, displacement ellipsoids at 30%. For clarity, hydrogen atoms, apart from the bridging hydrides and those attached to C30 and C30<sup>1</sup> are omitted, as are the minor components of disordered atoms and solvent. Dipp groups are displayed as wireframe, also for visual ease. Selected bond lengths (Å): Ca1–N1 2.3237(17), Ca1–N2 2.3253(16), Ca1–Zn1 3.0196(5), Ca1–Zn1<sup>1</sup> 3.0188(5), Ca1–C30 2.608(2), Ca1–C31<sup>1</sup> 2.629(2), Ca1–H1 2.37(3), Ca–H1<sup>1</sup> 3.40(2), Zn1–C30 2.038(2), Zn1–C31 2.047(3), Zn1–H1 1.79(3), Zn1–H1<sup>1</sup> 1.78(3), Zn1–Zn1<sup>1</sup> 2.7222(5). Symmetry operations to generate primed atoms:  $^1 1 - x, 1 - y, 1 - z$ .

compared to Ca1–H1. Nevertheless, both Zn–H distances are commensurate with precedented molecular zinc compounds comprising bridging hydrides (*ca.* 1.6–1.8 Å).<sup>22–26</sup>

Although atoms in molecules (AIM) analysis of **3** (PBE0/def2-TZVPP//TPSS/def2-SVP level, see the ESI $^\dagger$  for full details) reveals an appreciable Zn1–H1 ( $\rho(r) = 0.0630$ ,  $\nabla^2\rho(r) = +0.1620$ ,  $\text{H}(r) = -0.0129$ ) bond critical point (BCP), with Ca1–H1 ( $\rho(r) = 0.0214$ ,  $\nabla^2\rho(r) = +0.0623$ ,  $\text{H}(r) = 0.0003$ ), this is comparatively weaker in nature with respect to those characterized in **1** ( $\rho(r) = 0.0326$ ,  $\nabla^2\rho(r) = +0.0835$ ,  $\text{H}(r) = -0.0017$ ), indicating transfer of each hydride to Zn upon addition of  $\text{ZnMe}_2$ . This deduction is further supported by mechanistic calculations (see the ESI $^\dagger$  for more details). The Zn1–C30 BCP ( $\rho(r) = 0.0870$ ,  $\nabla^2\rho(r) = +0.2180$ ,  $\text{H}(r) = -0.0242$ ), while slightly weaker with respect to  $\text{ZnMe}_2$  ( $\rho(r) = 0.1140$ ,  $\nabla^2\rho(r) = +0.2100$ ,  $\text{H}(r) = -0.0453$ ), is still significantly stronger than Ca1–C30 ( $\rho(r) = 0.0242$ ,  $\nabla^2\rho(r) = +0.0957$ ,  $\text{H}(r) = +0.0199$ ) which, along with Natural Bond Orbital analysis, indicates this structure is best ascribed as a dianionic  $\{\text{Zn}_2\text{Me}_2\text{H}_2\}^{2-}$  hydridomethylzincate(*n*) charge-compensated by flanking  $\{(\text{BDI})\text{Ca}\}^+$  cations.

Although compound **3** is sufficiently stable in solution to allow the prompt acquisition of NMR spectra (Fig. S3–S6, ESI $^\dagger$ ), a further intramolecular transformation was apparent upon redissolution at ambient temperature in  $d_8$ -toluene. After 2 hours the resultant  $^1\text{H}$  NMR spectrum (Fig. S7, ESI $^\dagger$ ) comprised an approximate 1:4 ratio of compounds **2** and **3** along with a further minor species (**4**), which was most clearly identified by the emergence of a broad upfield methyl resonance at  $-1.35$  ppm. Reasoning that the breadth of this latter signal was most likely a consequence of its dynamic consumption to form **2** (Scheme 3), a further reaction was performed between **1** and a sub-stoichiometric amount (0.5 eq.) of  $\text{ZnMe}_2$ . Under these conditions, compound **4** was observed as the major





Scheme 3 Proposed reaction pathway between  $\text{ZnMe}_2$  and  $[(\text{BDI})\text{CaH}]_2$  (**1**), at ambient temperature.

product after 2 hours (Fig. S8, ESI<sup>†</sup>). Removal of volatiles at this point, followed by extraction into hexane and immediate crystallization at  $-35^\circ\text{C}$ , thus, provided a pure sample of compound **4** in the form of colourless crystals.

A solution of **4** in  $\text{C}_6\text{D}_6$  displays single BDI  $\gamma$ -methine and Dipp *isopropyl* methine resonances in its  $^1\text{H}$  NMR spectrum at 4.74 and 3.07 ppm, respectively, indicative of a symmetrical species. Although somewhat downfield in comparison to the methyl resonance assigned to the THF-adduct of  $[\text{CaMe}_2]_\infty$ ,  $[(\text{THF})_{10}\text{Ca}_7\text{Me}_{14}]$  ( $-1.42$  ppm),<sup>8</sup> consistent with its exclusive binding to the more electropositive calcium, the now sharp (3H) resonance of **4** at  $\delta_{\text{H}} -1.29$  ( $\delta_{\text{C}} 8.3$  ppm) is significantly upfield with respect to the metallomethyl signal of **3**. The constitution of compound **4** was ultimately confirmed by X-ray diffraction analysis, which established it as a centrosymmetric dimer in the solid state (Fig. 2).

The dimeric  $\text{Ca}-\mu_2-\text{C}-\text{Ca}$  structure of **4** is reminiscent of previously described longer-chain  $\sigma$ -alkyl calcium derivatives in which each calcium centre is similarly ligated by a bidentate BDI ligand.<sup>12,13</sup> Both the  $\text{Ca1}-\text{C30}$  [ $2.500(3)$  Å] and  $\text{Ca1}-\text{C30}^1$  [ $2.539(2)$  Å] bond lengths in **4**, however, are notably shorter than in any higher homologue (e.g.  $[(\text{BDI})\text{CaEt}]_2$   $2.5733(19)$  Å).<sup>6,12,13</sup> Similarly, the contacts between the methyl carbon and the 4-coordinate calcium atom in **4** are shorter than the analogous three-centre  $\text{Ca}-\mu_2-\text{C}-\text{Ca}$  bonds in Anwender's structurally characterised derivative,  $[(\text{THP})_5\text{Ca}_3(\text{Me})_5(\text{I})]$  (THP = tetrahydropyran) [ $2.592(8)$ – $2.673(9)$  Å],<sup>8</sup> in which the calcium centres reside in a 6-coordinate *pseudo*-octahedral geometry, and the small number of heterometallic  $\text{Ca}-\mu_2-\text{Me}-\text{Al}$ -containing species that have been described.  $[(\text{Ca}(\mu_2-\text{Me})_2\text{AlMe}_2)_2(\text{Phen})]$  (Phen = 1,10-phenanthroline)  $2.571(7)$ – $2.610(7)$  Å,<sup>27</sup>  $[(\text{Me}_5\text{C}_5)_2\text{Ca}(\mu_2-\text{Me}_3\text{Al}(\text{THF}))_2]$   $2.948(7)$ – $2.999(7)$  Å,<sup>28</sup> and  $[(\text{THF})_4\text{Ca}(\mu_2-\text{NR})(\mu_2-\text{Me})\text{AlMe}_2]$  R = Dipp  $2.651(2)$  Å,  $\text{SiPh}_3$   $2.668(2)$  Å.<sup>29</sup> The hypothetical linear  $\text{MeCaI}$  molecule has been predicted to display a terminal  $\text{Ca}-\text{C}$  bond as short as  $2.377$  Å,<sup>2b</sup> while the analogous metric in gas phase dimethylcalcium itself had earlier been computed to be  $2.487$  or  $2.416$  Å, dependant on the adoption of a linear or bent geometry, respectively.<sup>30,31</sup> While these estimates most likely represent unapproachable extremes, it is notable that the most closely comparable  $\text{C}-\text{Ca}$  bond lengths are provided by Anwender's 5-coordinate calcium complexes,  $(\text{Tp}^{\text{Bu},\text{Me}}\text{Ca}(\text{Me})(\text{THF}))$  ( $2.477(2)$ ,  $2.482(2)$  Å) and  $[(\text{Tp}^{\text{Bu},\text{Me}}\text{Ca}(\text{Me})(\text{THP}))]$ , ( $2.485(2)$ ,  $2.507(2)$  Å), which provide unique examples of terminal calcium-to-methyl interactions.<sup>8</sup> Complementary AIM analysis of **4** was subsequently

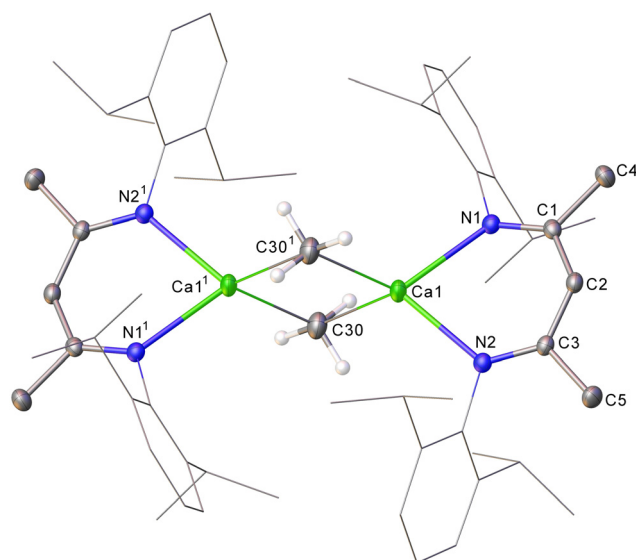


Fig. 2 Molecular structure of **4**, displacement ellipsoids at 30%. For clarity, an occluded molecule of hexane and the hydrogen atoms, apart from those attached to  $\text{C30}/\text{C30}^1$ , are omitted and the Dipp groups are displayed as wireframe. Selected bond lengths (Å) and angles ( $^\circ$ ):  $\text{Ca1}-\text{N1}$   $2.3285(15)$ ,  $\text{Ca1}-\text{N2}$   $2.3299(15)$ ,  $\text{Ca1}-\text{C30}$   $2.500(3)$ ,  $\text{Ca1}-\text{C30}^1$   $2.539(2)$ ,  $\text{N1}-\text{Ca1}-\text{N2}$   $81.53(5)$ ,  $\text{N1}-\text{Ca1}-\text{C30}$   $120.58(7)$ ,  $\text{N1}-\text{Ca1}-\text{C30}^1$   $120.70(7)$ . Symmetry operations to generate primed atoms:  $^11 - x, 1 - y, 2 - z$ .

undertaken (PBE0/def2-TZVPP//TPSS/def2-SVP), revealing a suite of similar  $\text{Ca}-\text{C}$  BCPs ( $\rho(r) = 0.0339/0.0338$ ,  $\nabla^2\rho(r) = +0.1100/+0.0990$ ,  $\text{H}(r) = -0.0011/-0.0004$ ) and computed atomic charges ( $q_{\text{Ca1}} = +1.593$ ,  $q_{\text{C30}} = -0.640$ ), which are indicative of bridging methyl interactions dominated by electrostatic character.

In summary, we have shown that the reaction between  $\text{ZnMe}_2$  and **1** proceeds in a step-wise manner, affording the bimetallic hydrido-zincate complex, **3**. Although, under appropriate conditions, the intermediates **3** and **4** can be isolated exclusively, compound **3** undergoes a subsequent intramolecular transformation to afford **4** and, ultimately, **2**. We suggest that **2** is the thermodynamic product of an equilibration process that is rendered irreversible as a consequence of the insoluble polymeric nature of  $[\text{Ca}(\text{H})\text{Me}]_\infty$  (Scheme 3). Compound **4** corrects a notable omission from the homologous series of  $\beta$ -diketiminato alkylcalcium derivatives and we are currently exploring its reactivity and its potential as a potent methylating agent.



The authors acknowledge the EPSRC (EP/X01181X/1) and the University of Bath's Research Computing Group (doi.org/10.15125/b6cd-s854) for their support in this work.

## Data availability

Experimental details, NMR spectra, X-ray crystallography, computational details, and atomic coordinates for the optimized geometries of the compounds can be found in the ESI.† Crystallographic data for all compounds have been deposited with the Cambridge Crystallographic Data Centre as supplementary publications CCDC 2360310 and 2360311 for **3** and **4**, respectively. Copies of these data can be obtained free of charge on application to CCDC.

## Conflicts of interest

There are no conflicts to declare.

## Notes and references

- (a) V. Grignard, *C. R. Hebd. Seances Acad. Sci.*, 1900, **130**, 1322; (b) D. Seyferth, *Organometallics*, 2009, **28**, 1598–1605.
- (a) S. Harder, *Alkaline-Earth Metal Compounds: Oddities and Applications*, Springer, 2013; (b) M. Westerhausen, A. Koch, H. Görls and S. Krieck, *Chem. Eur. J.*, 2017, **23**, 1456–1483.
- E. Beckmann, *Chem. Ber.*, 1905, **38**, 904–906.
- H. Gilman and F. Schulze, *J. Am. Chem. Soc.*, 1926, **48**, 2463–2467.
- F. G. N. Cloke, P. B. Hitchcock, M. F. Lappert, G. A. Lawless and B. Royo, *J. Chem. Soc., Chem. Commun.*, 1991, 724–726.
- See for example, (a) C. Eaborn, S. A. Hawkes, P. B. Hitchcock and J. D. Smith, *Chem. Commun.*, 1997, 1961–1962; (b) F. Feil and S. Harder, *Organometallics*, 2000, **19**, 5010–5015; (c) S. Harder, F. Feil and A. Weeber, *Organometallics*, 2001, **20**, 1044–1046; (d) M. R. Crimmin, A. G. M. Barrett, M. S. Hill, D. J. MacDougall, M. F. Mahon and P. A. Procopiou, *Chem. Eur. J.*, 2008, **14**, 11292–11295; (e) M. P. Coles, S. E. Sözerli, J. D. Smith, P. B. Hitchcock and I. J. Day, *Organometallics*, 2009, **28**, 1579–1581; (f) M. S. Hill, M. F. Mahon and T. P. Robinson, *Chem. Commun.*, 2010, **46**, 2498–2500; (g) A. Koch, M. Wirgenings, S. Krieck, H. Görls, G. Pohnert and M. Westerhausen, *Organometallics*, 2017, **36**, 3981–3986.
- (a) M. Westerhausen, M. Gärtner, R. Fischer and J. Langer, *Angew. Chem., Int. Ed.*, 2007, **46**, 1950–1956; (b) R. Fischer, H. Görls and M. Westerhausen, *Inorg. Chem. Commun.*, 2005, **8**, 1159–1161; (c) R. Fischer, M. Gärtner, H. Görls and M. Westerhausen, *Angew. Chem., Int. Ed.*, 2006, **45**, 609–612; (d) R. Fischer, M. Gärtner, H. Görls and M. Westerhausen, *Organometallics*, 2006, **25**, 3496–3500; (e) M. Westerhausen, M. Gärtner, R. Fischer and J. Langer, *Angew. Chem., Int. Ed.*, 2007, **46**, 1950–1956; (f) M. Westerhausen, M. Gärtner, R. Fischer, J. Langer, L. Yu and M. Reiher, *Chem. Eur. J.*, 2007, **13**, 6292–6306; (g) J. Langer, H. Görls and M. Westerhausen, *Inorg. Chem. Commun.*, 2007, **10**, 853–855; (h) J. Langer, S. Krieck, H. Görls and M. Westerhausen, *Angew. Chem., Int. Ed.*, 2009, **48**, 5741–5744; (i) S. Krieck, H. Görls and M. Westerhausen, *Chem. Asian J.*, 2010, **5**, 272–277; (j) R. Fischer, J. Langer, S. Krieck, H. Görls and M. Westerhausen, *Organometallics*, 2011, **30**, 1359–1365; (k) J. Langer, M. Kohler, R. Fischer, F. Dundar, H. Görls and M. Westerhausen, *Organometallics*, 2012, **31**, 6172–6182; (l) M. Kohler, J. Langer, H. Görls and M. Westerhausen, *Organometallics*, 2012, **31**, 8647–8653; (m) J. Langer, M. Kohler, H. Görls and M. Westerhausen, *Chem. Eur. J.*, 2014, **20**, 3154–3161; (n) M. Kohler, J. Langer, H. Görls and M. Westerhausen, *Organometallics*, 2014, **33**, 6381–6388; (o) A. Koch, S. Krieck, H. Görls and M. Westerhausen, *Organometallics*, 2017, **36**, 2811–2817; (p) A. Koch, S. Krieck, H. Görls and M. Westerhausen, *Dalton Trans.*, 2018, **47**, 12534–12539; (q) J. Langer, M. Kohler, J. Hildebrand, R. Fischer, H. Görls and M. Westerhausen, *Angew. Chem., Int. Ed.*, 2013, **52**, 3507–3510.
- B. M. Wolf, C. Stuhl, C. Maichle-Mössmer and R. Anwender, *J. Am. Chem. Soc.*, 2018, **140**, 2373–2383.
- See, for example, (a) S. Harder, F. Feil and K. Knoll, *Angew. Chem., Int. Ed.*, 2001, **40**, 4261–4264; (b) S. Harder and F. Feil, *Organometallics*, 2002, **21**, 2268–2274; (c) F. Feil, C. Müller and S. Harder, *J. Organometal. Chem.*, 2003, **683**, 56–63; (d) D. F.-J. Piesik, K. Habe and S. Harder, *Eur. J. Inorg. Chem.*, 2007, 5652–5661; (e) A. Causero, H. Elsen, G. Ballmann, A. Escalona and S. Harder, *Chem. Commun.*, 2017, **53**, 10386–10389; (f) X. Shi, C. Hou, L. Zhao, P. Deng and J. Cheng, *Chem. Commun.*, 2020, **56**, 5162–5165; (g) L. Zhao, X. Shi and J. Cheng, *ACS Catal.*, 2021, **11**, 2041–2046.
- For benzylic derivatives, see (a) M. R. Crimmin, A. G. M. Barrett, M. S. Hill, D. J. MacDougall, M. F. Mahon and P. A. Procopiou, *Dalton Trans.*, 2009, 9715–9717; (b) X. Zheng, I. del Rosal, X. Xu, Y. Yao, L. Maron and X. Xu, *Inorg. Chem.*, 2021, **60**, 5114–5121.
- S. Harder and J. Brettar, *Angew. Chem., Int. Ed.*, 2006, **45**, 3474–3478.
- A. S. S. Wilson, M. S. Hill, M. F. Mahon, C. Dinoi and L. Maron, *Science*, 2017, **358**, 1168–1171.
- (a) A. S. S. Wilson, M. S. Hill and M. F. Mahon, *Organometallics*, 2019, **38**, 351–360; (b) A. S. S. Wilson, C. Dinoi, M. S. Hill, M. F. Mahon and L. Maron, *Angew. Chem., Int. Ed.*, 2018, **57**, 15500–15504.
- K. G. Pearce, C. Dinoi, M. S. Hill, M. F. Mahon, L. Maron, R. J. Schwamm and A. S. S. Wilson, *Angew. Chem., Int. Ed.*, 2022, **61**, e202200305.
- K. G. Pearce, C. Dinoi, R. J. Schwamm, L. Maron, M. F. Mahon and M. S. Hill, *Adv. Sci.*, 2023, **10**, 2304765.
- R. W. Siegler, D. W. Nierenberg and W. F. Hickey, *Hum. Pathol.*, 1999, **30**, 720–723.
- J. Prust, A. Stasch, W. Zheng, H. W. Roesky, E. Alexopoulos, I. Usón, D. Böhler and T. Schuchardt, *Organometallics*, 2001, **20**, 3825–3828.
- K. G. Pearce, L. J. Morris, T. P. Robinson, A. L. Johnson, M. F. Mahon and M. S. Hill, *Dalton Trans.*, 2024, **53**, 6653–6659.
- M. R. Crimmin, M. S. Hill, P. B. Hitchcock and M. F. Mahon, *New J. Chem.*, 2010, **34**, 1572–1578.
- A. Causero, G. Ballmann, J. Pahl, C. Färber, J. Intemann and S. Harder, *Dalton Trans.*, 2017, **46**, 1822–1831.
- M. Westerhausen, C. Gückel, H. Piotrowski and M. Wogt, *Z. Anorg. Allg. Chem.*, 2002, **628**, 735–740.
- A. Hicken, A. J. P. White and M. R. Crimmin, *Inorg. Chem.*, 2017, **56**, 8669–8682.
- H. Hao, C. Cui, H. W. Roesky, G. Bai, H.-G. Schmidt and M. Noltemeyer, *Chem. Commun.*, 2001, 1118–1119.
- A. Rit, T. P. Spaniol, L. Maron and J. Okuda, *Organometallics*, 2014, **33**, 2039–2047.
- M. Chen, S. Jiang, L. Maron and X. Xu, *Dalton Trans.*, 2019, **48**, 1931–1935.
- A. Lennartson, M. Håkansson and S. Jagner, *Angew. Chem., Int. Ed.*, 2007, **46**, 6678–6680.
- O. Michel, C. Meermann, K. W. Törnroos and R. Anwender, *Organometallics*, 2009, **28**, 4783–4790.
- P. S. Tanner, R. A. Williams and T. P. Hanusa, *Inorg. Chem.*, 1993, **32**, 2234–2235.
- B. M. Wolf, C. Maichle-Mössmer and R. Anwender, *Angew. Chem., Int. Ed.*, 2016, **55**, 13893–13897.
- M. Kaupp and P. V. R. Schleyer, *J. Am. Chem. Soc.*, 1992, **114**, 491–497.
- I. Bytheway, R. J. Gillespie, T.-H. Tang and R. F. W. Bader, *Inorg. Chem.*, 1995, **34**, 2407–2414.

